Role of miR-138 on Radio Sensitivity of Gastric Carcinoma Cells and Its Molecular Mechanism

Yibo Zhang
Tan Lu
Min Yuan
Liying Chen
Yuting Liu
Cui Cui
Bo Sun
Cunzhi Feng

To explore FOXP4 and miR-138 in gastric carcinoma (GC) and its related mechanisms. Sixty-eight GC patients from January 2018 to January 2019 were selected as group A, and 66 healthy people as group B. GC cells and gastric mucosal epithelial cells were purchased, sh-FOXP4, si-FOXP4, NC, miR-138-inhibitor, and miR-138-mimics were transfected into MKN-45 and NCI-N87 cells. The FOXP4 and miR-138 expression levels in samples were tested by qRT-PCR, and N-cadherin, vimentin, Fibronectin, Slug, E-Cadherin and γ-catenin downstream proteins in cells were detected by WB. The proliferation was tested by MTT assay, invasion was tested by Transwell assay, and apoptosis was detected by flow cytometry assay. FOXP4 was highly expressed in GC, miR-138 was poorly expressed in GC, and AUC of FOXP4 and miR-138 was > 0.8. FOXP4 and miR-138 were tied to the age, gender, tumor invasion, differentiation degree, tumor location and TNM stage of GC patients. Silent expression of FOXP4 and overexpression of miR-138 can promote apoptosis, inhibit cell growth and epithelial-mesenchymal transition (ETM). The two also can inhibit N-cadherin, vimentin, Fibronectin and Slug proteins, and promote E-Cadherin and γ-catenin. Dual luciferase report confirmed that FOXP4 and miR-138 had targeted relationship. In terms of radiological parameters, the SF_2 and D_0 (Gy) values of transfected miR-138mimic+pcDNA3. 1-FOXP4 were dramatically higher than those of transfected miR-138mimic+pcDNA3. 1 cells, and SER was lower than those of transfected miR-138 mimic+ pcDNA3. 1 cells (P<0.05), suggesting FOXP4 partially adjusted the radiosensitization role of miR-138. In conclusion, miR-138 can regulate EMT of GC cells by adjusting FOXP4 and enhance radiosensitivity of those cells.

Keywords: gastric carcinoma (GC), miR-138, FOXP4, radiosensitivity, biological function

Tob Regul Sci.™ 2021;7(5-1):4304-4313

DOI:doi.org/10.18001/TRS.7.5.1.208

INTRODUCTION

Gastric carcinoma (GC) is a malignant digestive system neoplasm of gastric mucosa epithelium. With the change of people's diet structure and some bad eating habits, GC tends to be younger (1). Early GC has no obvious symptoms and is confirmed at the advanced stage. The resection rate for advanced GC is low and the mortality is high (2). At present, GC patients in different stages are treated through surgical treatment, radiotherapy and chemotherapy, molecular targeted therapy, immunotherapy and supportive therapy. With the continuous

Yibo Zhang Outpatient Department of Wound Ostomy, Weifang People's Hospital, Weifang 261041, China, Tan Lu Ward 2 (Gastroenterology), Department of General Surgery, Binzhou People's Hospital Affiliated to Shandong First Medical University, Binzhou 256600, China, Min Yuan Department of Nursing, Weifang People's Hospital, Weifang 261041, China, Liying Chen Department of Nursing, Weifang People's Hospital, Weifang 261041, China, Yuting Liu Department of Dentistry, Weifang People's Hospital, Weifang 261041, China, Cui Cui Ward 2, Department of Neurology, Yidu Central Hospital of Weifang, Qingzhou 262500, China, Bo Sun Department of Vascular Surgery, Weifang People's Hospital, Weifang 261041, China, Cunzhi Feng Ward 2 (Gastroenterology), Department of General Surgery, Binzhou People's Hospital Affiliated to Shandong First Medical University, Binzhou 256600, China, *Corresponding author: Department of Nursing, Weifang People's Hospital, No. 151 Guangwen Street, Weifang 261041, China (E-mail: eegsu0@163.com)*

development of molecular targeted therapy, relevant biomarkers have been confirmed to determine the occurrence, development, prognosis and potential mechanism of GC, thus making more appropriate plans for its treatment (3,4). In recent years, some studies have found that microRNA (miRNA) affects EMT of GC cells and changes in biological functions of carcinoma cells, and miRNA expression is tied to its occurrence and development (5).It participates in various biological steps of tumors and has diagnostic and prognostic effect for tumors (6-9). A large number of studies reveal that compared with healthy people, miRNA in carcinoma has abnormal expression. However, the molecular mechanism of FOXP4 and GC is still unclear (10,11). At the moment, studies have found that miRNA genes related to carcinoma cells can affect tumor invasiveness by regulating EMT (12-14). Wang et al. found that miRNA partially regulated the survival of hepatocellular carcinoma cells by targeting relevant transcription factors of FOXP family and miR-338-3p by downregulating FOXP4. Targeting miR-338-3p/FOXP4 axis may be a new therapeutic scheme for hepatic cellular carcinoma(15). However, the role of miR-138 on radiosensitivity of GC cells and its molecular mechanism are still unclear.

Therefore, we explored its effect on radiosensitivity of GC cells and its molecular mechanism in order to find reliable tumor markers and potential drug targets for clinical diagnosis and prognosis.

MATERIALS AND METHODS

Patients

Sixty-eight GC patients from January 2018 to January 2019 were collected as group A, and 66 healthy people who came to our hospital for physical examination at the same time were taken as group B. There was no remarkable difference in gender, age and other aspects between A and B ($P>0.05$), which was comparable. Inclusion criteria were as below: those confirmed as GC by pathology, cytology and imaging (16); GC patients who did not receive relevant preoperative chemotherapy, immunotherapy and radiotherapy. Exclusion criteria were as below: those complicated with liver cirrhosis and coagulation dysfunction; those with incomplete general clinical data; those who did not cooperate with follow-up; those with less than 1 month expected survival time; those lost to be followed up. The study was approved by the Ethics Committee, and patients have signed informed consent forms in advance.

Main Instruments and Reagents

MKN-45, NCI-N87, MGC-803, AZ521 human GC cell line and GES 1 normal human gastric mucosa epithelial cells (BNCC337682, BNCC100416, BNCC100665, BNCC338085, BNCC337969) were bought from BeNa Culture Collection. Besides, ABI Stepone Plus real-time fluorescence quantitative PCR, Lipofectamine™2000 transfection, Trizol extraction, Annexin V/PI apoptosis detection kit (Invitrogen), SYBR Green PCR Master Mix (Applied Biosystems), MTT kit (Beyotime Biotechnology Co., Ltd., Product Number: C0008), 10% FBS, penicillin-streptomycin mixed solution (100× double antibody), DMEM, Transwell kit (GibcoTM BRL), β-catenin polyclonal goat IgG, cyclin D1 polyclonal goat IgG, c-myc polyclonal goat IgG, β-actin, horseradish peroxidase (HRP) labeled goat anti-mouse secondary antibody (R&D Systems), ECL chemiluminescence kit, BCA protein kit, Multiskan™ GO full wavelength microplate reader (Thermo Fisher), FACSCanto (Becton Dickinson), DR5000 (BioRad). All primer sequences were synthesized by Sangon Biotech.

Detection Methods

Sample collection: 5 mL of elbow venous blood from GC patients and healthy people were collected, centrifuged 10 min at 3000×g, and the serum was placed for follow-up use.

1.3.1 Cell culture and transfection experiments

GC cell lines were transfected into DMEM medium including 10% FBS and penicillin-streptomycin mixed medium, and placed in a 5% CO_2, 36 ℃ constant temperature saturated humidity cell incubator. FOXP4-siRNA (si-FOXP4), FOXP4-shRNA (sh-FOXP4) and empty plasmid (siRNA-NC) were transfected referring to the instruction manual of Lipofectamine™2000. Primers were transfected into the cells with the greatest difference in FOXP4. Six hours after transfection, they were placed in a culture solutionincluding 10% FBS in depth. Their transfection efficiency was verified by qRT-PCR.

qRT-PCR detection

mRNA in serum and cells was tested by qRT-PCR. Total RNA in serum was extracted and dissolved in 20 μL DEPC water referring Trizol reagent, and then reverse transcribed. The reaction was as follows: M-MLV 1 μl, Olig(d T) 1 μl, RNA enzyme inhibitor 0.5 μl, d NTPs 1 μl, RNase freewater made up to 15 μl. The cellswere then placed 60 min at 38℃. We took 1 μl c DNA and placed it at 85℃ for 5 s. The synthesized c DNA was employed as a template for qRT-PCR amplification. The PCR reaction was prepared: 10×PCR buffer 2.5 μl, d NTPs 1 μl, upstream and downstream primers 1 μl each, Taq DNA polymerase 0.25 μl, dd H_2O supplemented to 25 μl. Reaction steps were as follows: pre-denaturation 85℃ for 15 min, denaturation 85℃ for 15 s, annealing 58℃ for 30 s, a total of 35 cycles, a

final extension at 62℃ for 15 min. Each sample was supplied with 3 multiple wells. miR-138 employed U6 as internal reference and FOXP4 employed GAPDH as internal reference, the amplification curve and melting curve were determined after the reaction, and the relative amount of the target gene was calculated according to the result parameters. The target gene was calculated by $2^{-\Delta Ct}$. Primer sequences are shown in Table 1.

Table 1.
miR-26b-8p, FOXP4 and their internal reference primer sequences

Genes	Forward primer	Reverse primer
miR-138	5′-AGCTGGTGTTGTGAATC-3′	5'-GTGCAGGGTCCGAGGT-3'
FOXP4	5'-CGACATGATGGTGGAATCTG-3'	5'-TGTTTGCTGTCATTGTTCCC-3'
U6	5'-CTCGCTTCGGCAGCACA-3'	5'-AACGCTTCACGAATTTGCGT-3'
GAPDH	5'-CAAAGGTGGATCAGATTCAAG-3'	5'-GGTGAGCATTATCACCCAGAA-3'

Western blot test

The cells were obtained to a centrifuge tube, centrifuged 10 min at 4 ℃, 12000×g, the supernatant was collected as protein sample, and the protein was tested by BCA. Lysis buffer was supplemented to dilute the protein sample to 20 mg/ml, and 8.00% separation gel and 5.00% lamination gel were applied. It was under SDS-PAGE electrophoresis and moved to PVDF. βcatenin, cyclin D1, c-myc (1:1000) primary antibody, and internal reference βactin (1:3000) were supplemented, and then it was sealed all night long at 4 ℃. HRP labeled sheep anti-mouse secondary antibody (1: 5000) was supplemented, and then it was incubated 1 h at 36℃ and rinsed 3 times with TBST for 5 min each time. Soon afterwards, it was developed in dark room using enhanced chemiluminescence (ECL), and excess liquid on the membrane was absorbed. The protein bands were observed, and the gray values were testedby Quantity One software (Molecular Devices Corp).

Cell proliferation experiment

Cell viability was tested by MTT. Cells were harvested 24 h after transfection. Cell density was adjusted to 5×10^3 cells/well. They were inoculated on 86-well plates and incubated 24, 48 and 62 h respectively at 36℃. Altogether 20 μL MTT (5 μmg/mL) was supplemented at each time point. They were continuously cultured 4 h at 36℃. Altogether 200 μL dimethyl sulfoxide was added. Then OD values were tested at 560 mm wavelength by spectrophotometer.

Transwell invasion experiment

Matrigel glue was coated in Transwell chamber and allowed to stand 30 min at 36℃. Cells were resuspended in serum-free DMEM culture with a cell density of 4×10^5 cells /mL. Altogether 200 μL of cell suspension was putinto the upper chamber and 800 μL of DMEM into the lower chamber. Then they were placed 24-48 h again. We took out the chamber, fixed them with 4% paraformaldehyde, and dyed them with 0.1% crystal violet and wiped those in the upper chamber. Ten high power fields were obtained to count the cells passing through the basement membrane of the chamber, indicating the cell invasion ability.

Apoptosis experiment

Cells transfected for 48 h were reacted with 0.25% trypsin, rinsed twice with PBS, resuspended with AnnexinV-binding buffer 100 μL, configured as 1×10^6 cells/mL suspension, supplemented with 5 μLAnnexin-V/FITC, and placed 15 min at 4℃. We added 5 μl PI staining solution and incubated them 5 min at 4℃. Flow cytometry was employed for detection. The test was repeated 3 times and results were averaged.

Irradiation treatment and grouping of cells

The cells were divided into miR-138mimic+pcDNA3.1, miR-138mimic+pcDNA3.1-FOXP4, miR-NC+pcDNA3.1-FOXP4, and empty plasmid miR-NC+pcDNA3. 1 groups based on the cell transfection scheme. Forty-eight hours after transfection, the cells of various transfection combinations were irradiated with radiation, and the radiobiological parameters, cell survival fraction (SF_2), average lethal dose D_0 (Gy) and radiosensitization ratio (SER) of those in each group were detected by colony forming experiment.

Statistical Methods

SPSS 20.0 (SPSS, Inc., Chicago, IL, USA) was applied for analysis. Normal distribution data were represented by meas±SD, and the comparison of measurement data applied independent-samples T test. Multiple time points comparison was conducted by ANOVA, and back testing by

Bonferroni. Comparison of mean values among multiple groups was under one-way ANOVA, and back testing was under LSD-t test. The diagnostic value was tested by ROC curve. Pearson test was applied to correlation. P<0.05 indicated a significant difference.

RESULTS

miR-138 and FOXP4 in Serum of GC Patients

After detecting FOXP4 and miR-138, we found that the FOXP4 in group A was dramatically higher than that in group B, while miR-13 in group A was dramatically lower than that in group B (P<0.001). Pearson test revealed that FOXP4 and miR-138 in the serum of GC patients had a negative correlation (P<0.001). AUC of FOXP4 and miR-138 were both > 0.8, 0.883, 0.850 by plotting ROC curve. (Figure 1)

Figure 1.
Expression and clinical value of FOXP4 and miR-138 in serum of GC patients.

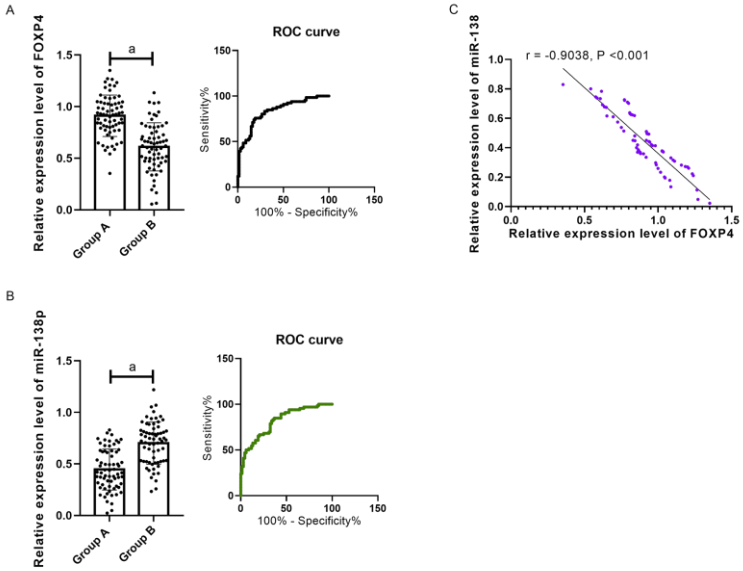

A: FOXP4 in group A was dramatically higher than that in group B, and it was highly expressed in serum of GC patients. AUC of FOXP4 >0.8. a means P<0.001.

B: miR-138 in group A was dramatically lower than that in group B, and it expressed low in GC patients. AUC of miR-138 >0.8. a means P<0.001.

C: FOXP4 and miR-138 were negatively correlated (r=-0.9038, P<0.001). a means P<0.001.

Expression of FOXP4 and miR-138 and Their Effects on Biological Functions of Cells

miR-138 was tested by qRT-PCR. Compared with GES 1 gastric mucosal epithelial cells, miR-138 in MKN-45 and NCI-N87 cells was dramatically down-regulated (P<0.05). We selected MKN-45 and NCI-N87 with the greatest expression difference for transfection. miR-138 in the miR-138-inhibitor group was dramatically lower than that in the miR-NC group (P<0.01), and it in the miR-138-mimics group was dramatically higher than that in the miR-NC group (P<0.01). CCK-8 results manifested that the proliferation of the miR-138-mimics group was obviously lower than that of the miR-NC group (P<0.05), and the proliferation of the miR-138-inhibitor group was obviously up-regulated than that of the miR-NC group (P<0.05). Flow cytometry revealed that the apoptosis of the miR-138-mimics group was dramatically higher than that of the miR-NC group (P<0.001), and the apoptosis of the miR-138-inhibitor group was dramatically lower than that of the miR-NC group (P<0.001). Transwell experiment manifested that the invasion of the miR-138-mimics group was obviously lower than that of the miR-NC group (P<0.001), and the invasion of the miR-138-inhibitor group was obviously higher than that of the miR-NC group (P<0.001). (Figure 2)

Figure 2.
miR-138 expression and its biological function (A)

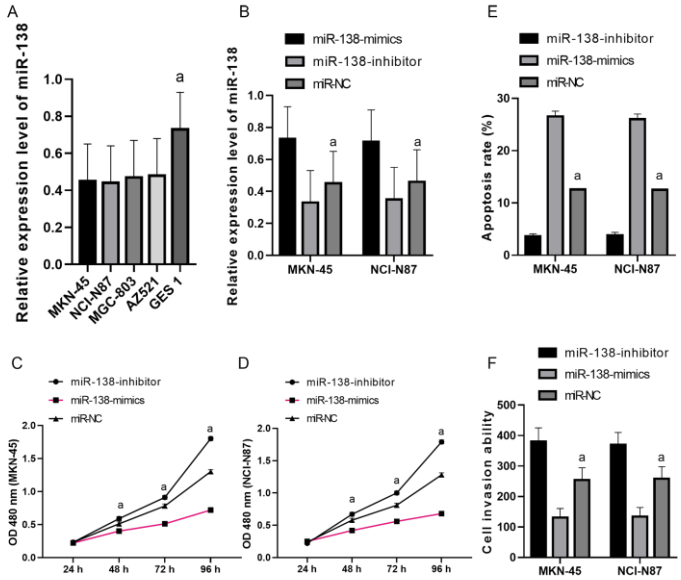

miR-138 expression after transfecting MKN-45 and NCI-N87 cells (B) proliferation of MKN-45 (C) and NCI-N87 (D) cells after transfection apoptosis of MKN-45 and NCI-N87 cells after transfection (E) invasion of MKN-45 and NCI-N87 cells after transfection (F)
Note: a means P<0.001.

FOXP4 was tested by qRT-PCR. Compared with GES 1 gastric mucosal epithelial cells, FOXP4 in MKN-45 and NCI-N87 up-regulated markedly (P<0.05). We selected MKN-45 and NCI-N87 cells with the greatest difference in expression for transfection. Compared with GES 1 gastric mucosal epithelial cells, the FOXP4 expression in MKN-45 and NCI-N87 cells increased remarkably (P<0.05). MKN-45 and NCI-N87 with the greatest expression difference were chosen for transfection. FOXP4 in the siRNA-FOXP4 was dramatically lower than that in the siRNA-NC (P<0.01), and it in the shRNA-FOXP4 was dramatically higher than that in the siRNA-NC (P<0.01). MTT results manifested that the proliferation of the siRNA-FOXP4 was obviously lower than that of the siRNA-NC (P<0.05), and the proliferation of the shRNA-FOXP4 was up-regulated than that of the siRNA-NC (P<0.05). Flow cytometry signified that the apoptosis of the siRNA-FOXP4 was dramatically lower than that of the siRNA-NC (P<0.001), and that of the shRNA-FOXP4 was dramatically lower than that of the siRNA-NC (P<0.001). Transwell experiment results manifested that the cell invasion ability of the siRNA-FOXP4 was obviously lower than that of the siRNA-NC (P<0.001), and the cell invasion ability of the shRNA-FOXP4 was obviously higher than that of the siRNA-NC (P<0.001). (Figure 3)

Figure 3.
FOXP4 expression and its biological function of cells

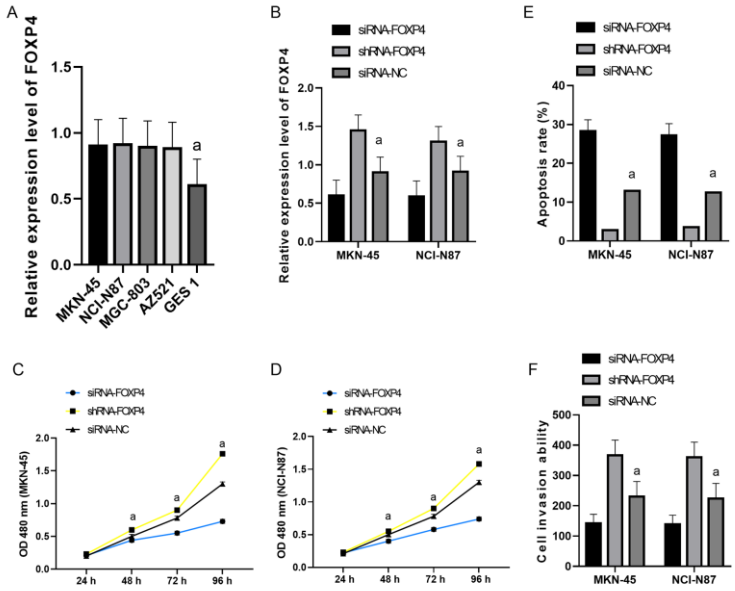

FOXP4 in each cell line (A)
FOXP4 expression after transfecting MKN-45 and NCI-N87 (B)
proliferation of MKN-45 (C) and NCI-N87 (D) after transfection
apoptosis of MKN-45 and NCI-N87 after transfection (E)
invasion of MKN-45 and NCI-N87 after transfection (F)
Note: a means P<0.001.

Effect of miR-138 Expression on EMT Mechanism of GC Cells

Western Blot results revealed that: Compared with N-cadherin, vimentin, Fibronectin and Slug proteins in transfected siRNA-NC cells, the sh-FOXP4 expression was dramatically up-regulated, while that of E-Cadherin and γ-catenin was dramatically down-regulated. However, after transfecting si-FOXP4, N-cadherin, vimentin, Fibronectin and Slug protein in siRNA-NC cells were obviously down-regulated, and the E-Cadherin and γ-catenin expression levels increased markedly (P<0.001).

Compared with miR-138-inhibitor cells, the E-Cadherin and γ-catenin expression levels were dramatically up-regulated. However, N-cadherin, vimentin, Fibronectin and Slug protein in transfected miR-138-mimics were obviously lower than that in transfected miR-NC cells, and the E-Cadherin and γ-catenin expression levels increased dramatically (P<0.001). (Figure 4)

Figure 4.
influence of FOXP4 and miR-138 on EMT

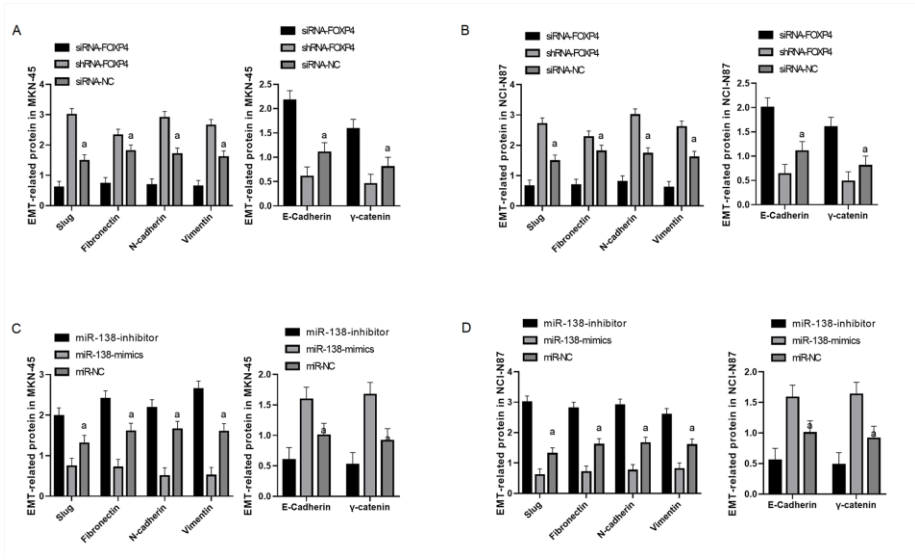

A: Compared with siRNA-NC, N-cadherin, vimentin, Fibronectin and Slug protein in transfected sh-FOXP4 cells were dramatically up-regulated, and E-Cadherin was dramatically down-regulated, while N-cadherin, vimentin, Fibronectin and Slug protein in Si-FOXP4 were obviously down-regulated, and E-Cadherin was obviously enhanced (MKN-45 cells).

B: The results were the same as A (NCI-N87 cell).

C: Compared with miR-NC, N-cadherin, vimentin, Fibronectin and Slug protein in transfected miR-138-inhibitor cell were dramatically up-regulated, and the E-Cadherin expression was dramatically down-regulated. However, the expression levels of N-cadherin, vimentin, Fibronectin and Slug protein in transfected miR-138-mimics cells was remarkably down-regulated, and the E-Cadherin expression was remarkably up-regulated (MKN-45 cells).

D: The results were the same as C (NCI-N87 cells).

Note: a indicates comparison with NC group (P<0.001).

Identification of Target Genes

To further verify the relationship between miR-138 and FOXP4, the target gene downstream of miR-138 was tested by Targetscan6.2, and a targeted binding site was found between miR-138 and FOXP4. Hence, we applied a dual luciferase activity test and it was revealed that pmirGLO-FOXP4-3'UT Wt luciferase activity reduced dramatically after miR-138 over-expression (P<0.001), but it had no influence on pmirGLO-FOXP4-3'UTR Mut luciferase activity (P>0.05). PCR detection signified that FOXP4 in MKN-45 and NCI-N87 was dramatically reduced after transfection of miR-138-mimics, and it in MKN-45 and NCI-N87 was dramatically up-regulated after transfection of miR-138-inhibitor (P<0.001) (Figure 5)

Figure 5.
Dual-luciferase activity assay

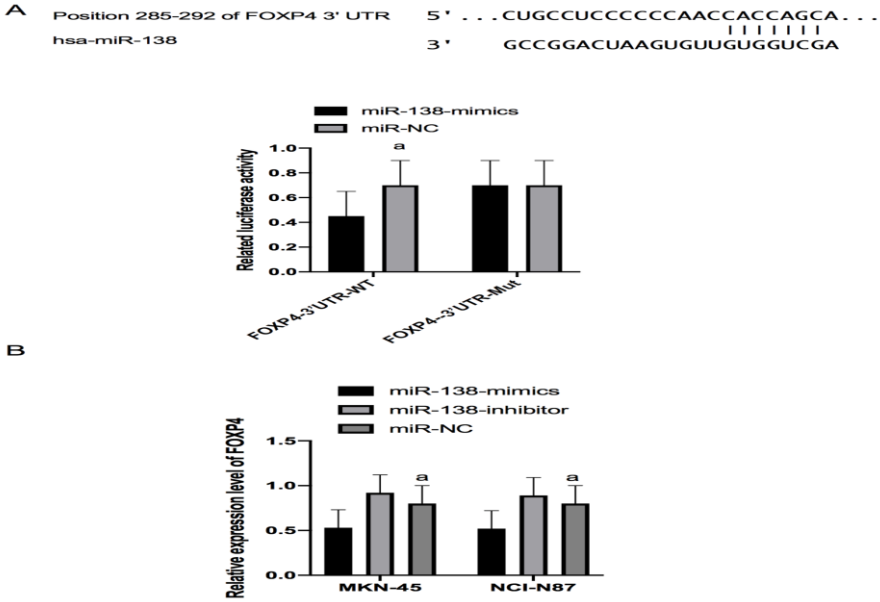

A: There is a binding site between miR-138 and FOXP4, and the results of relative luciferase activity-dual luciferase report assay are shown.

B: FOXP4 in MKN-45 and NCI-N87 after transfection

Note: a means P<0.001.

Role of miR-138 in Increasing Radiosensitivity of GC MKN-45 Cells Is Tied to Partial Mediation of FOXP4

In terms of radiological parameters, the SF_2 value and D_0 (Gy) value of transfected miR-138mimic+pcDNA3. 1-FOXP4 were dramatically higher than those of transfected miR-138mimic+pcDNA3.1 cells. SER transfected with miR-138mimic+ pcDNA3. 1-FOXP4 was smaller than cells transfected with miR-138 mimic+pcDNA3. 1, but was still significantly higher than those of miR-NC+pcDNA3. 1-FOXP4 and miR-NC+pcDNA3. 1 group (P<0.05), suggesting FOXP4 partially reversed the radiosensitization effect of miR-138. (Table 2)

Table 2.
Radiation parameters of GC MKN-45 cells

Group	SF_2	D_0（Gy）	SER
miR-138mimic+ pcDNA3. 1	0.532	2.603	1.66
miR-138mimic+pcDNA3.1-FOXP4	0.640	3.813	1.25
miR-NC+pcDNA3. 1-FOXP4	0.788	4.601	1.10
miR-NC+pcDNA3. 1	0.812	4.987	1.02

DISCUSSION

Gastric carcinoma (GC) is a worldwide public health problem. Radiotherapy plays a vital part in treating unresectable gastrointestinal carcinoma(17). At present, the progress of preoperative and postoperative radiotherapy for GC is continuous, but the inherent radioresistance of cells leads to the failure of radiotherapy for many patients. Improving the effectiveness of radiotherapy is a momentous goal of GC treatment at this stage (18). miRNA is a non-coding RNA involved in gene expression regulation of human life activities. Recently, as a new molecular target related to diseases, miRNA's clinical research and development has attracted much attention (19). Malla et al. found that miRNA might be the target of radiotherapy for carcinoma. They also confirmed that miRNA expression could predict the response of prostate carcinoma patients to radiotherapy, which was indicated as a potential target for improving radiotherapy (20). miR-138 is abnormally expressed in GC, and its radiosensitivity to GC and the interaction of related mechanisms are still unclear (21).

First, the FOXP4 expression was monitored by qRT-PCR. It was showed that miR-138 was abnormally reduced in the serum of GC patients, while FOXP4 was abnormally up-regulated. We further found that the low miR-138 and high FOXP4 had a correlation with the differentiation degree, stage and lymph node metastasis of GC patients through correlation analysis of their clinical and pathological characteristics. At present, reports have shown that miRNA can target downstream gene pairs to adjust cell biological functions (22). We further found that there was a targeting correlation of miR-138 with FOXP4 through the analysis of the TargetScan database. miR-138 plays a vital regulatory part in the process of tumor development and differentiation. At the moment, miR-138-5P has been proved to regulate GC cell cycle (23). Then we detected the TCGA database and the miR-138 and FOXP4 expression levels in GC cells. The results revealed that FOXP4 was enhanced and miR-138 was reduced in MKN-45 and NCI-N87, which was the same as the results of this research, indicating that FOXP4 and miR-138 both might play regulatory roles in GC.

In the cell experiment of this study, we compared human GC cell lines MKN-45 and NCI-N87 with GES 1 gastric mucosal epithelial cells respectively, and found that FOXP4 was enhanced and miR-138 was reduced in GC cell lines. Subsequently, we treated FOXP4 and miR-138 in MKN-45 and NCI-N87 by silencing and over-expression. The results signified that we further transfected sh-FOXP4, si-FOXP4, miR-138-mimics, miR-138-inhibitor sequences into MKN-45 and NCI-N87. Observing the cell biological function, we found that FOXP4 inhibited expression, and the proliferation and invasion after overexpression of miR-138 were dramatically inhibited. The occurrence and development are relevant to EMT. EMT will promote the biological function changes of tumor cells (24). This suggests that miR-138 can be used as a potential target for GC treatment. Inhibiting FOXP4 can hinder the proliferation, invasion and EMT of GC cells, which further suggests the influence of FOXP4 changes on GC. However, it has doubt about how FOXP4 affects the biological function of GC cells and EMT.

Studies have shown the correlation between EMT and radioresistance of carcinoma cells (25). Xie et al. pointed out that the radiosensitizing role of miR-1275 in esophageal carcinoma was attributed to the negative adjustment of miR-1275 on EMT of esophageal carcinoma cells (26). In this research, we observed EMT-related proteins after inhibiting or overexpressing miR-138 and FOXP4 in GC cells, and found that EMT-related proteins in those with high miR-138 and low FOXP4 were negatively regulated. This shows that miR-138 induces EMT by targeting FOXP4, thus promoting the radiosensitivity of carcinoma cells. However, overexpression of miR-138 saved FOXP4 from up-regulating damaged EMT, thus reducing the sensitivity of GC cells to radiation. There are also studies related to radiosensitivity of other carcinomas, which show that miR-9-5p targets SOCS5 to promote proliferation of cervical carcinoma cells, while affecting EMT and radiosensitivity of cervical carcinoma(27). We further verified the correlation of miR-18a-3 with FOXP4 through dual luciferase report, and discovered that the FOXP4-3'UT Wt luciferase activity increased dramatically after miR-138 was overexpressed, but it had no effect on FOXP4-3'UTR Mut luciferase activity. The miR-138 expression in transfected si-FOXP4 increased markedly, which suggested that there was a targeted regulatory relationship between FOXP4

and miR-138. Finally, we found that inhibiting FOXP4 can promote miR-138 expression, thus affecting the biological mechanism of GC cells.

We found that overexpression of FOXP4 could weaken the radiosensitizing effect of miR-138 through certain transfection combination and subsequent apoptosis analysis, while overexpression of miR-138 and FOXP4 would reduce the apoptosis rate of GC cells after irradiation compared with those that overexpressed miR-138 alone. This shows that the sensitivity of GC cells to radiation indeed increases by overexpressing miR-138 and inhibiting FOXP4, but not only FOXP4, there must be other miR-138 target genes involved in this process, which is worthy of further study.

In this research, we have proved that miR-138 is under-expressed in GC, and overexpression of miR-138 can inhibit FOXP4-mediated radiation sensitivity of GC cells and EMT molecular mechanism. Nevertheless, we still have certain limitations, and further research is needed on whether miR-138 can affect tumor occurrence and development through other ways. Therefore, we hope that in future research, we can explore the regulatory network of miR-138 through bioinformatics analysis to provide more basis for our experiments.

Overall, miR-138 can adjust EMT of GC cells by adjusting FOXP4, and enhance their radiosensitivity.

REFERENCES

1. Guilford PJ, Holyoake AJ. Markers for detection of gastric carcinoma. U.S2019; Patent 10, 179, 935.
2. Rugge M, Sugano K, Scarpignato C, Sacchi D, Oblitas WJ, Naccarato AG. Gastric carcinoma prevention targeted on risk assessment: Gastritis OLGA staging. Helicobacter 2019; 24: e12571.
3. Rugge M, Meggio A, Pravadelli C Gastritis staging in the endoscopic follow-up for the secondary prevention of gastric carcinoma: a 5-year prospective study of 1755 patients. Gut 2019; 68: 11-17.
4. Seidlitz T, Merker SR, Rothe A. Human gastric carcinoma modelling using organoids. Gut 2019; 68: 207-217.
5. Wang R, Sun Y, Yu W Downregulation of miRNA-214 in carcinoma-associated fibroblasts contributes to migration and invasion of gastric carcinoma cells through targeting FGF9 and inducing EMT. J Exp Clin carcinoma Res 2019; 38: 20.
6. Ding H, Shi Y, Liu X, Qiu A. MicroRNA-4513 Promotes Gastric carcinoma Cell Proliferation and Epithelial–Mesenchymal Transition Through Targeting KAT6B. Hum Gene Ther Clin Dev 2019; 30: 142-148.
7. Huang L, Wang ZY, Pan DD. Penicillin- binding protein 1A mutation- positive Helicobacter pylori promotes epithelial- mesenchymal transition in gastric carcinoma via the suppression of microRNA- 134. Int J Oncol 2019; 54: 916-928.
8. Hang C, Yan HS, Gong C, Gao H, Mao QH, Zhu JX. MicroRNA- 9 inhibits gastric carcinoma cell proliferation and migration by targeting neuropilin- 1. Exp Ther Med 2019; 18: 2524-2530.
9. Quan X, Chen D, Li M, Chen X, Huang M. MicroRNA- 150- 5p and SRC kinase signaling inhibitor 1 involvement in the pathological development of gastric carcinoma. Exp Ther Med 2019; 18: 2667-2674.
10. Zhang X, Sai B, Wang F Hypoxic BMSC-derived exosomal miRNAs promote metastasis of lung carcinoma cells via STAT3-induced EMT. Mol carcinoma2019; 18: 40.
11. Liu S, Wang L, Li Y, Cui Y, Wang Y, Liu C. Long non-coding RNA CHRF promotes proliferation and mesenchymal transition (EMT) in prostate carcinoma cell line PC3 requiring up-regulating microRNA-10b. Biol Chem 2019; 400: 1035-1045.
12. Wang H, Wei H, Wang J, Li L, Chen A, Li Z. MicroRNA-181d-5p-Containing Exosomes Derived from CAFs Promote EMT by Regulating CDX2/HOXA5 in Breast carcinoma. Mol Ther Nucleic Acids 2020; 19: 654-667.
13. Feng T, Zhu Z, Jin Y The microRNA- 708- 5p/ZEB1/EMT axis mediates the metastatic potential of osteosarcoma. Oncol Rep 2020; 43: 491-502.
14. Chen J, Zhong Y, Li L. miR-124 and miR-203 synergistically inactivate EMT pathway via coregulation of ZEB2 in clear cell renal cell carcinoma (ccRCC). J Transl Med 2020; 18: 69.
15. Wang G, Sun Y, He Y, Ji C, Hu B, Sun Y. MicroRNA-338-3p inhibits cell proliferation in hepatocellular carcinoma by target forkhead box P4 (FOXP4). Int J Clin Exp Pathol 2015; 8: 337-344.
16. Li J, Zhang B, Cui J, Liang Z, Liu K. Mir-203 inhibits the invasion and emt of gastric carcinoma cells by directly targeting annexin a4. Oncol Res 2019; 27: 789-799.
17. Datta J, Da Silva EM, Kandoth C Poor survival after resection of early gastric carcinoma: extremes of survivorship analysis reveal distinct genomic profile. Br J Surg 2020; 107: 14-19.
18. Jayanathan M, Erwin RP, Molacek N MAGIC versus MacDonald treatment regimens for gastric carcinoma: Trends and predictors of multimodal therapy for gastric carcinoma using the National carcinoma Database. Am J Surg 2020; 219: 129-135.
19. Xie M, Dart DA, Guo T. MicroRNA-1 acts as a tumor suppressor microRNA by inhibiting angiogenesis-related growth factors in human gastric carcinoma. Gastric carcinoma2018; 21: 41-54.
20. Malla B, Zaugg K, Vassella E, Aebersold DM, Dal Pra A. Exosomes and exosomal microRNAs in prostate carcinoma radiation therapy. Int J Radiat Oncol Biol Phys 2017; 98: 982-995.
21. Gao W, Lam JW, Li JZ MicroRNA-138-5p controls sensitivity of nasopharyngeal carcinoma to radiation by targeting EIF4EBP1. Oncol Rep 2017; 37:

913-920.
22. Cortez MA, Anfossi S, Ramapriyan R Role of miRNAs in immune responses and immunotherapy in carcinoma. Genes Chromosomes carcinoma2019; 58: 244-253.
23. Ning J, Jiao Y, Xie X. miR- 138- 5p modulates the expression of excision repair cross- complementing proteins ERCC1 and ERCC4, and regulates the sensitivity of gastric carcinoma cells to cisplatin. Oncol Rep 2019; 41: 1131-1139.
24. Li S, Cong X, Gao H Tumor-associated neutrophils induce EMT by IL-17a to promote migration and invasion in gastric carcinoma cells. J Exp Clin carcinoma Res 2019; 38: 6.
25. Wang W, Xiong Y, Ding X Cathepsin L activated by mutant p53 and Egr-1 promotes ionizing radiation-induced EMT in human NSCLC. J Exp Clin carcinoma Res 2019; 38: 61.
26. Xie C, Wu Y, Fei Z, Fang Y, Xiao S, Su H. MicroRNA - 1275 induces radiosensitization in oesophageal carcinoma by regulating epithelial - to - mesenchymal transition via Wnt/β- catenin pathway. J Cell Mol Med 2020; 24: 747-759.
27. Wei YQ, Jiao XL, Zhang SY, Xu Y, Li S, Kong BH. MiR-9-5p could promote angiogenesis and radiosensitivity in cervical carcinoma by targeting SOCS5. Eur Rev Med Pharmacol Sci 2019; 23: 7314-7326.